

(1A1) has undergone successive bifurcations from a limit cycle (fixed point) to a two-torus (limit-cycle) to a three-torus (two-torus) to chaos. As just mentioned, the last bifurcation may involve a preliminary frequency locking. The occurrence of a quasiperiodic motion with three incommensurate frequencies just prior to the onset of a chaotic regime has previously been observed in Bénard convection experiments.<sup>7</sup> To our knowledge, this is the first instance in which such a sequence of bifurcations arises in numerical simulations of partial differential equations. According to Newhouse, Ruelle, and Takens,<sup>8</sup> perturbations of a three-torus can produce strange axiom-A attractors. The present results suggest that a three-frequency motion can actually be stable for a finite interval of values of the control parameter  $q$ .

We wish to thank Dr. J. D. Farmer for many helpful discussions. This work was supported by

the National Science Foundation under Grants No. CME-7916162 and No. MEA-8114780.

<sup>1</sup>A. C. Newell and J. A. Whitehead, *J. Fluid Mech.* **38**, 279 (1969).

<sup>2</sup>S. Kogelman and R. C. DiPrima, *Phys. Fluids* **13**, 1 (1970).

<sup>3</sup>K. Stewartson and J. T. Stuart, *J. Fluid Mech.* **48**, 529 (1971).

<sup>4</sup>H. C. Yuen and B. M. Lake, *Ann. Rev. Fluid Mech.* **12**, 303 (1980).

<sup>5</sup>J. T. Stuart and R. C. DiPrima, *Proc. Roy. Soc. London, Sect. A* **362**, 27 (1978).

<sup>6</sup>B. Fornberg and G. B. Whitham, *Philos. Trans. Roy. Soc. London* **289**, 373 (1978).

<sup>7</sup>J. P. Gollub and S. V. Benson, *J. Fluid Mech.* **100**, 449 (1980).

<sup>8</sup>S. Newhouse, D. Ruelle, and F. Takens, *Commun. Math. Phys.* **64**, 35 (1978).

## Sequence of Instabilities in Electromagnetically Driven Flows between Conducting Cylinders

P. Tabeling

*Laboratoire de Génie Electrique de Paris, F-91190 Gif-sur-Yvette, France*

(Received 23 February 1982)

An experiment on electromagnetically driven flows shows sequences of instabilities involving overstability and slow oscillations of the cellular structure before the onset of turbulence.

PACS numbers: 47.65.+a, 47.25.-c

Transition to turbulence in hydromagnetic Taylor-vortex flows of liquid metal has not received much attention until now. This situation contrasts with the hydrodynamic case (no magnetic field) for which extensive experimental data exist.<sup>1</sup> On physical grounds the effect of an imposed external magnetic field on cellular flows is expected to alter profoundly the sequence of events leading to turbulence. The present Letter is related to a limited experimental investigation of Taylor instability subjected to an external magnetic field.

Figure 1 shows the experimental arrangement. The mercury is confined between two "long" copper cylinders, 3.84 cm in height, and 8.0 and 8.22 cm in diameter, respectively; a thin layer of nickel (25  $\mu\text{m}$ ) and gold (2–3  $\mu\text{m}$ ) has been deposited on the copper surfaces so that the electri-

cal and mechanical conditions of the flow are well defined on the boundaries. The duct is axially

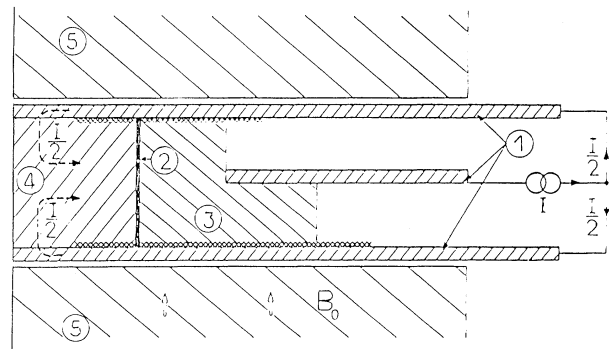


FIG. 1. The experimental arrangement. 1, alloy aluminum plates; 2, mercury; 3, outer copper cylinder; 4, inner copper cylinders; 5, electromagnet.

limited by two circular Mylar sheets which serve as insulating end walls. A net current  $I$ , directed radially, flows through the duct. The electromagnet is a 300-mm polar piece, with a distance of 50 mm between the poles. The liquid metal is driven by the interaction of the axially applied magnetic field  $B_0$  and the radial current  $I$  flowing through the duct. The total driving force  $B_0 Id$  is equivalent to a transverse pressure gradient  $K = B_0 Id / 2\pi R_1 L$ , in which  $R_1$  is the inner cylinder radius,  $d$  is the gap, and  $L$  is the height of the duct. The ranges of the accessible values for  $I$  and  $B_0$  are 0–1000 A and 0–1.3 T, respectively, all being better than  $10^{-4}$  regulated. The spatially averaged velocity of the flow is deduced from the measurements of the total voltage drop between the two conducting cylinders.<sup>2</sup> Time-dependent local voltages are also measured by means of four small electrodes placed on the outer cylinder. Those electrodes detect velocity fluctuations without mechanically perturbing the flow. Because of the relative positions of such probes, the phase measurements between them give information on the spatial structure of the flow. The typical values of voltage fluctuations  $\Delta\varphi$  lie in the range 0.1 to 3  $\mu\text{V}$ ; they are amplified by a low-noise transformer (1:100 wiring ratio). The resulting background noise figure, as observed in the experiments, is about  $10^{-3}$  while the lower frequency limit for reasonable measurements is 0.02 Hz. The amplified signal is registered and treated on a Hewlett-Packard model 3582 A fast-Fourier-transform spectrum analyzer.

We shall now describe the experimental results restricting ourselves to the range  $0.93 \text{ T} < B_0 \leq 1.25 \text{ T}$ .<sup>3</sup> For all the runs, the external magnetic field  $B_0$  is kept constant, while the current  $I$  is gradually varied, either continuously or stepwise. The low values of  $I$  correspond to the steady laminar state; the definition of this state is now

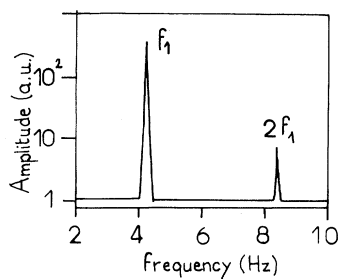


FIG. 2. Fourier analysis of the fluctuating voltage at the output of a wall probe obtained at  $B_0 = 1.1 \text{ T}$  and  $I = 45.750 \text{ A}$ .

well understood both theoretically and experimentally<sup>4</sup>; the velocity field is purely circumferential; the shape of the velocity profile is parabolic throughout the duct and decreases to zero in thin Hartmann layers near the insulating end plates; when  $I$  is increased, a first instability occurs in the form of oscillatory disturbances, with frequency  $f_1$  (see Fig. 2). The transition from the steady to the time-dependent state is sharp and reversible. Above the instability point, we have observed a strict phase locking between the four probes. The phase measurements indicate that this instability has the form of a wave traveling in both the axial (vertical) and azimuthal directions. This should correspond to spiraling vortices. In all the cases, the azimuthal phase velocity of the wave slightly exceeds the mean velocity of the flow. The dependence of frequency  $f_1$  on the external magnetic field  $B_0$  is shown in Fig. 3. In the range  $0.95 \leq B_0 \leq 1.14 \text{ T}$ , the azimuthal wave number  $m$  of the disturbance is 4 while it is 3 at larger values of  $B_0$ ; this reveals a change in the preferred unstable mode when  $B_0$  is increased above 1.14 T. The amplitude  $A_1$  of the disturbance close to the threshold is represented in Fig. 4 as a function of the discrepancy  $\epsilon = Re/Re_1 - 1$ , where  $Re = B_0 Id^2 / 4\pi R_1 L \eta \nu$  is the Reynolds number and  $Re_1$  is the critical value of  $Re$  (where  $\eta$  and  $\nu$  are the viscosity and kinematic viscosity of the fluid, respectively). We obtain a Landau-type dependence for the amplitude which shows that the observed bifurcation is normal. The physical origin of this bifurcation is overstability since its onset occurs for values of the Reynolds number lower than those corresponding to the onset of stationary disturbances.<sup>5</sup> The occurrence of overstability in magnetohydrodynamic Taylor-vortex flows between conducting cylinders had previously been predicted by several authors. The value of  $B_0$  above which the oscillatory dis-

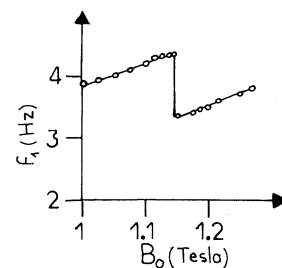


FIG. 3. Frequency  $f_1$  of the first oscillatory mode as a function of the external magnetic field  $B_0$ .

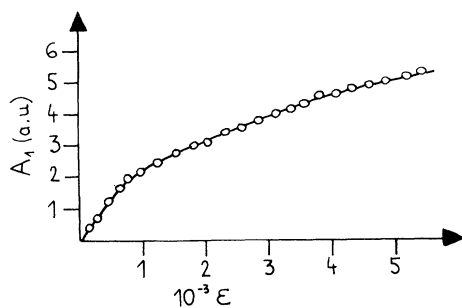


FIG. 4. The maximum amplitude  $A_1$  of the oscillatory mode as a function of the discrepancy  $\epsilon = Re/Re_1 - 1$ , at  $B_0 = 1.2$  T.

turbances are more critical than the stationary ones is in good agreement with the results of Volkov, Gurfink, and Poluektov<sup>6</sup> (they give 0.92 T), although the curvature ratio that they considered is significantly larger ( $d/R_1 = 0.316$  in Ref. 6 to be compared with  $d/R_1 = 0.026$  in the present experiment).

The phase measurements between a couple of probes located at the same angular position but at two distinct values of the vertical coordinate indicate an abrupt decrease of the optimal axial wave number from the state  $m=4$  to  $m=3$ . The number of cells which we have deduced from such measurements decreases from 60 to 15 in the range  $0.93 < B_0 \leq 1.25$  T. We further note that, even when the number of cells is large, a strict phase locking is observed between the four probes. This suggests that the stabilizing effect of the magnetic field on the cellular structure is strong. The phase measurements also indicate a continuous decrease of the axial wave number above threshold at any value of  $B_0$  above 0.93 T.

We now turn to the second bifurcation of the flow: Figure 5 represents five direct recordings of the potential fluctuation obtained for  $B_0 = 1.215$  T. At  $\epsilon = 4 \times 10^{-3}$  the flow oscillates at frequency  $f_1 = 0.60$  Hz. As  $\epsilon$  is raised up above  $4.5 \times 10^{-3}$  a new frequency  $f_2 = 0.056$  Hz appears in the form of an amplitude modulation of  $f_1$ . Further increases of  $\epsilon$  lead to an increase of the amplitude of the low-frequency signal together with its harmonic content. The frequency  $f_2$  depends on the initial conditions imposed on the system. Different increasing rates of  $\epsilon$  (or small stepwise increases) lead to values of  $f_2$  differing by 20%–30% from each other. This contrasts with the first bifurcation of the flow for which frequency  $f_1$  is not related to the initial conditions. The present spread of the values of  $f_2$  should be related to the

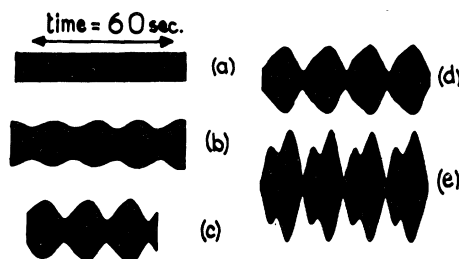


FIG. 5. Direct time recording of voltage fluctuations at different values of  $\epsilon$ , for  $B_0 = 1.215$  T. (a)  $\epsilon = 4 \times 10^{-3}$ , (b)  $\epsilon = 4.8 \times 10^{-3}$ , (c)  $\epsilon = 5.1 \times 10^{-3}$ , (d)  $\epsilon = 5.4 \times 10^{-3}$ , (e)  $\epsilon = 6.2 \times 10^{-3}$ .

nonuniqueness of the accessible states of the flow above the first instability point. Further information concerning the spatial structure of the flow is given by phase measurements: The two probes located at two distinct values of the angular coordinate reveal that the envelopes shown in Fig. 5 have the same phase. The origin of this instability remains to be understood.

When  $\epsilon$  is further increased, a new bifurcation occurs in the form of a superimposed velocity wave, involving a well-defined frequency  $f_1'$ . The ratio  $f_1'/f_1$  is about  $\frac{3}{4}$  in the range  $0.93 \text{ T} < B_0 \leq 1.14 \text{ T}$  and  $\frac{4}{3}$  at larger values of  $B_0$ ; accordingly the azimuthal wave number  $m'$  of the new velocity wave is respectively 3 and 4 in the above ranges of values of  $B_0$ . This new bifurcation should be related to a simple instability of the mean flow via nonaxisymmetric modes (because of the small values of  $\epsilon$ , the mean flow is slightly distorted by the nonlinear effects).

Figure 6 shows the transition to turbulence for  $B_0 = 1.2$  T, as generally observed in the experiments. When  $\epsilon = 12 \times 10^{-3}$  the state of the flow is pseudoperiodic with three basic frequencies  $f_1 = 3.52$  Hz,  $f_2 = 0.06$  Hz, and  $f_1' = 4.68$  Hz. The power spectrum of Fig. 6(a), approximately centered on  $f_1' - f_1$ , shows successive spectral lines in the form  $mf_1 \pm nf_1' \pm pf_2$ , where  $m$ ,  $n$ , and  $p$  are integers. A further increase in  $\epsilon$  leads to the emergence of broad bands in the spectrum, corresponding to the turbulent state.

The features described in the present Letter are in many respects similar to those found in dynamical systems with few degrees of freedom.<sup>7</sup> In the present experiment, the two modes  $f_1$  and  $f_1'$  have a simple physical origin (instability of the laminar primary flow via nonaxisymmetric oscillatory modes); however, the physical origin of the oscillator  $f_2$  is more difficult to under-

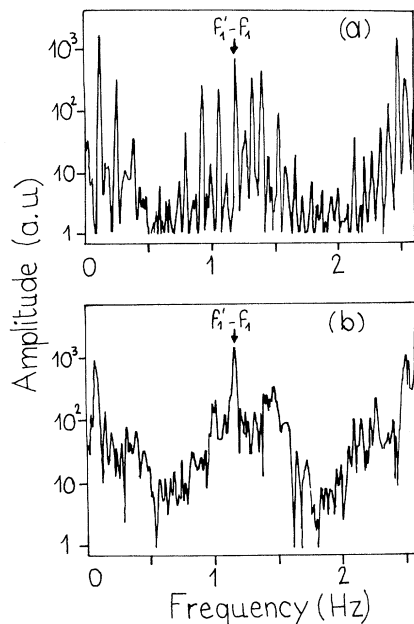


FIG. 6. Fourier analysis of the output voltage at  $B_0 = 1.2$  T. (a)  $\epsilon = 12 \times 10^{-3}$ , (b)  $\epsilon = 18 \times 10^{-3}$ .

stand. One is tempted to relate the onset of turbulence to the nonlinear dynamics of three coupled oscillators, in accordance with the general scheme of Ruelle and Takens.<sup>8</sup> However, an observer moving with the phase velocity  $2\pi f_1/m$  de-

fects only two independent frequencies so that this type of interpretation is questionable.

<sup>1</sup>P. R. Fenstermacher, H. L. Swinney, and J. P. Gollub, *J. Fluid Mech.* **94**, 103–128 (1979).

<sup>2</sup>Mean velocity measurements performed in a similar experiment have been previously reported by the author in *J. Fluid Mech.* **112**, 329–345 (1981).

<sup>3</sup>In the range  $0.3 < B_0 < 0.93$  T, the flow is turbulent at the first threshold: Slow aperiodic fluctuations of the velocity, weakly correlated in space, appear as the first dynamical event at the output of the probes. This phenomenon is probably due to continuous chaotic changes in the structure of stationary cells. More detailed investigation is clearly required.

<sup>4</sup>See J. A. Baylis and J. C. R. Hunt, *J. Fluid Mech.* **48**, 423 (1971); P. Tabeling and J. P. C. Chabrierie, *J. Fluid Mech.* **103**, 225 (1981).

<sup>5</sup>The onset of stationary cellular flow has been calculated by S. Chandrasekhar, *Hydrodynamic and Hydro-magnetic Stability* (Oxford Univ. Press, London, 1961), and P. Tabeling and J. P. Chabrierie, *Phys. Fluids* **29**, 406 (1981).

<sup>6</sup>T. S. Chang and W. K. Sartory, *Proc. Roy. Soc. Ser. A* **301**, 451–457 (1967); B. D. Hassard, T. S. Chang, and G. S. S. Ludford, *Plasma Phys.* **15**, 1235–1245 (1973); A. V. Volkov, M. M. Gurfink, and A. P. Poluektov, *Magnetohydrodynamika* **1**, 81 (1976).

<sup>7</sup>See, for instance, the experiment of J. P. Gollub and S. V. Benson, *J. Fluid Mech.* **100**, 409 (1980).

<sup>8</sup>D. Ruelle and F. Takens, *Commun. Math. Phys.* **20**, 167 (1971).

## Direct Measurement of the Fuel Density-Radius Product in Laser-Fusion Experiments

S. Kacenjari, S. Skupsky, A. Entenberg, L. Goldman, and M. Richardson

*Laboratory for Laser Energetics, University of Rochester, Rochester, New York 14627*

(Received 3 May 1982)

The first *direct* measurement of fuel density-radius product  $\rho R$  in laser-fusion experiments is obtained by measuring the number of deuterium and tritium ions elastically scattered out of the fuel by 14-MeV fusion neutrons. They were recorded with the solid-state track detector CR-39. The energy spectrum of these particles is found to agree well with the theoretical result. This diagnostic was used in low- and high-compression experiments and gave measured  $\rho R$  values of  $1.3 \times 10^{-4}$  and  $1.2 \times 10^{-3}$  g/cm<sup>2</sup>, with an uncertainty of  $\sim 20\%$ .

PACS numbers: 52.70.-m

The first *direct* measurement of fuel density-radius product  $\rho R$  in laser-fusion experiments has been obtained for the implosion of deuterium-tritium (DT) filled, glass-shell targets. (The quantity  $\rho R$  characterizes the proximity to energy breakeven in inertial fusion<sup>1</sup> and is analogous to  $n\tau$  used for the Lawson criterion in magnetic fu-

sion.) The measurement involved counting the number of energetic deuterons and tritons produced from elastic scattering with the 14-MeV DT fusion neutrons as they traversed the fuel (Fig. 1). These hydrogen isotopes can be recorded by the solid-state track detector CR-39.<sup>2</sup> The total number of "knockon" particles,  $Q$ , is related to